

Chapter 7

Chaotic Behavior of Orthogonally Projective Triangle Folding Map

Jun Nishimura and Tomohisa Hayakawa

7.1 Introduction

Chaotic behavior embedded in dynamical systems has been attracting huge attention in the field of nonlinear dynamical systems theory since 1960s. Wide variety of results have also been reported concerning chaotic systems in many areas such as fundamental field of physics and biology as well.

One of the major objectives of investigating chaos is to elucidate the mechanism of generating chaotic behavior. A mathematical approach to address analysis problems of chaotic systems is to observe simple nonlinear dynamics and find key factors that give rise to chaos. The simplicity of the nonlinear models to consider is central in obtaining better understanding of complicated behaviors. Notable examples of such relatively simple dynamic models are the logistic map, the tent map, the Horseshoe map [12, 13], to cite but a few (see also [1–5, 7–9, 11] and the references therein).

In our earlier paper [6], we considered a *simple* folding map for equilateral triangles (which we call the *triangle folding map*) that has sensitivity with respect to the initial conditions. The operation is shown in Fig. 7.1 and defined by the the following procedure:

- [1] Fold along NL and bring A to M.
- [2] Fold along LM and bring B to N.
- [3] Fold along MN and bring C to L.
- [4] Rotate LMN around its center by π radian.
- [5] Enlarge LMN by double so that MNL coincides with ABC.

Specifically, we provided fixed point analysis and periodic point analysis associated with this mapping operation by sequentially partitioning a restricted domain. Furthermore, we discussed some connections of the folding map to the Sierpinski gasket,

J. Nishimura · T. Hayakawa (✉)
Graduate School of Information Science and Engineering,
Tokyo Institute of Technology, 2-12-1 Oh-Okayama, Meguro-ku, Tokyo 152-8552, Japan
e-mail: hayakawa@mei.titech.ac.jp

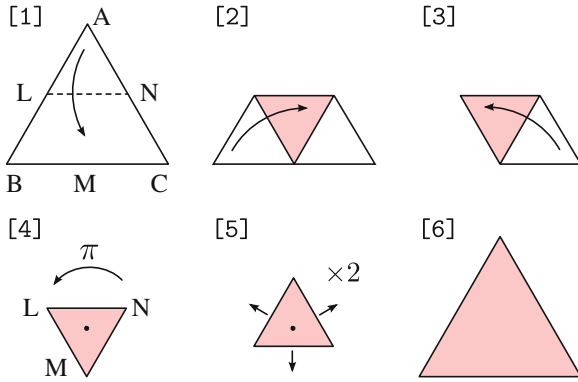


Fig. 7.1 Triangle folding map [6]. The map was defined as a surjective map

which is well known to be composed of self-homothetic triangles, and proposed a scheme to construct other interesting fractals by removing certain regions of the equilateral triangle.

In this article, we introduce a bifurcation parameter for the folding angle and generalize this triangle folding map so that the operation in [6] reduces to a special case of the new map. In particular, we call the operation the orthogonally projective triangle folding map and provide a similar analysis given in [6] in terms of the fixed points. We note that the preliminary results of this article can be found in [10].

7.2 Orthogonally Projective Triangle Folding Map

For the orthogonally projective triangle folding map, consider the equilateral triangle ABC given by [4] in Fig. 7.1. In order to introduce the bifurcation parameter in the folding operation, let θ be the folding angle in operation [2] and [3] in Fig. 7.1 and the sequence of operation is given by Fig. 7.2.

After the folding operation above, the resulting triangle in [5] becomes identical to the equilateral triangle in [1]. We denote this folding operation [1]–[5] by $F : \mathcal{T} \rightarrow \mathcal{T}$. For example, the point $P \in \mathcal{T}$ shown in [1] of Fig. 7.3 is mapped by

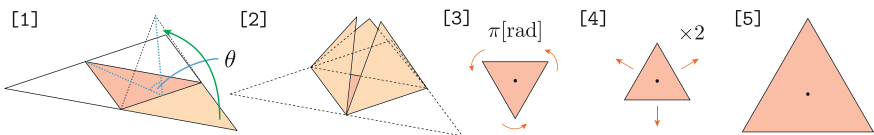


Fig. 7.2 Orthogonally projective triangle folding map. The triangle folding map in Fig. 7.1 is modified to introduce the bifurcation parameter θ . The case of $\theta = 0$ corresponding to the triangle folding map defined in Fig. 7.1

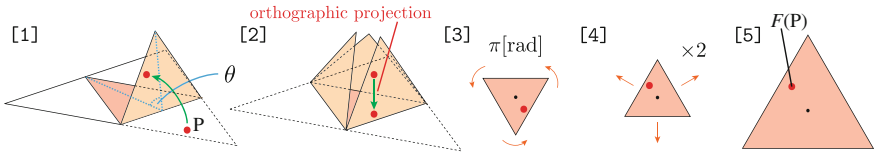


Fig. 7.3 Visualization of the mapping scheme for a given point in \mathcal{T} . This map will be redefined from the map from \mathcal{D} to \mathcal{D} as in Definition 7.1

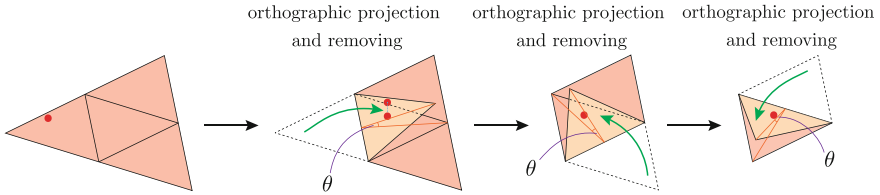


Fig. 7.4 Mapping with small θ

the function F to another point $F(P)$ in [5]. For the case where the folding angle θ is small, i.e., $\cos^{-1} \frac{1}{3} < \theta < \frac{\pi}{2}$, the operation is shown in Fig. 7.4. Note that the operation given by Fig. 7.1 corresponds to the case of $\theta = 0$. It is immediate that the map F is surjective as discussed below.

Now, it is important to note that there are several variations of prescribing the operation from [3] to [4] in Fig. 7.2 in order to define the surjective map from \mathcal{T} to \mathcal{T} . For example, by rotating the triangle by $\frac{\pi}{6}$ radian, instead of π radian, counterclockwise (or clockwise), we can obtain a similar map to the original map \mathcal{T} . Or, more easily, the triangle in [3] can be flipped upside down to arrive at [4] through which we can construct a surjective map from \mathcal{T} to \mathcal{T} . This commonality is due to the reflective and the rotational symmetry that the equilateral triangles possess and it is preferable to characterize the map that describes the essential dynamics of the folding operation. The following notion precludes the ambiguity of the operation F .

Definition 7.1 (*Equivalence relation on \mathcal{T}*) Consider the map $F : \mathcal{T} \rightarrow \mathcal{T}$ defined by Fig. 7.2. Two points $P, Q \in \mathcal{T}$ are considered to be equivalent if P is transformed to Q via rotation by $2\pi/3$ or $4\pi/3$ radians, or reflection with respect to the symmetric axis of the equilateral triangle, or the combination of the rotation and the reflection. Specifically, we denote by

$$\text{equiv } \mathcal{X} \triangleq \{t \in \mathcal{T} : t \text{ has the equivalence relation with a point in } \mathcal{X}\}, \quad (7.1)$$

the equivalence set associated with the set $\mathcal{X} \subset \mathcal{T}$.

Note that the center of the equilateral triangle has its equivalence relation with itself, and any point on the symmetric axis (except for the center) has 2 other points (on the other symmetric axes) that have equivalence relation with it. Otherwise, a point on \mathcal{T} has 5 other points that have equivalence relation to each other (see

Fig. 7.5 Equivalence relation for the triangle folding map. The 6 points in the left triangle is identified as the same point and hence the top left point (marked in red) in the left figure is considered as the point in \mathcal{D} in the right figure

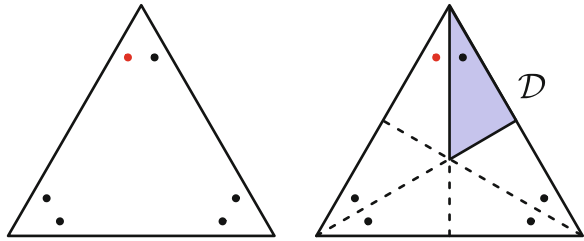


Fig. 7.6 Domain \mathcal{D} in the coordinate system

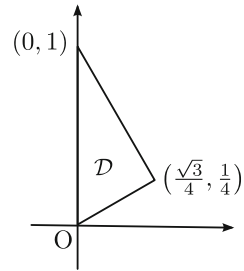


Fig. 7.5, left). In any case, it is important to note that any point $P \in \mathcal{T}$ has a *unique* point in \mathcal{D} that has the equivalence relation with P , where the closed subset $\mathcal{D} \subset \mathcal{T}$ is given by partitioning \mathcal{T} with the three symmetric axes (Fig. 7.5, right). Note that the 6 partitioned sets are right triangles and are all identical to each other in the shape and the size so that the choice of the partitioned set is not important.

Now, from the analysis above, we restrict the domain and the codomain into \mathcal{D} , instead of the original equilateral triangle \mathcal{T} , and define a new map $f : \mathcal{D} \rightarrow \mathcal{D}$ associated with the folding map F under the equivalence relation given by Definition 7.1. Note that for a point $R \in \mathcal{D}$, $f(R) \in \mathcal{D}$ has the equivalence relation with $F(R) \in \mathcal{T}$.

In order to describe the map f more clearly, we define the x - y coordinate system to the triangle. Specifically, let the length of the edges of \mathcal{T} be $2\sqrt{3}$ and, as shown in Fig. 7.6, let the center of the equilateral triangle be placed at the origin, and let the bottom edge be parallel to the x -axis. In this case, the map f is described by a piecewise affine function given in Definition 7.2 below.

For the statement of the following results, let the domain \mathcal{D} be further partitioned into the 4 closed subdomains \mathcal{D}_i , $i = 0, 1, 2, 3$, for the case of $0 \leq \theta < \cos^{-1} \frac{1}{3}$ as given by Fig. 7.7 (left) and the 2 closed subdomains \mathcal{D}_i , $i = 2, 3$, for the case of $\cos^{-1} \frac{1}{3} < \theta < \frac{\pi}{2}$ as given by Fig. 7.7 (right).

Definition 7.2 (*Orthogonally projective triangle folding map*) For the point $p = [x, y]^T$ in the closed domain $\mathcal{D} \subset \mathbb{R}^2$, the folding map $f^\theta : \mathcal{D} \rightarrow \mathcal{D}$ for the equilateral triangle is given by

$$f^\theta(p) \triangleq f_i^\theta(p), \quad p \in \mathcal{D}_i^\theta, \quad i = 0, 1, 2, 3, \tag{7.2}$$

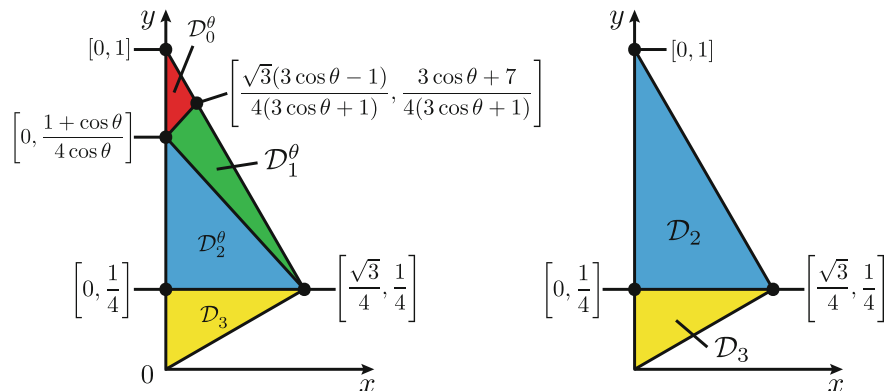


Fig. 7.7 Partitioned domains of \mathcal{D} with respect to θ ; (left) $0 \leq \theta < \cos^{-1} \frac{1}{3}$; (right) $\cos^{-1} \frac{1}{3} < \theta < \frac{\pi}{2}$. When $\theta \searrow \cos^{-1} \frac{1}{3}$, the domains \mathcal{D}_0^θ and \mathcal{D}_1^θ in the left figure degenerate

where

$$\begin{aligned}
 f_0^\theta(p) &\triangleq \begin{bmatrix} 2 & 0 \\ 0 & 2 \cos \theta \end{bmatrix} p - \frac{1 + \cos \theta}{4} \begin{bmatrix} 0 \\ 2 \end{bmatrix}, \\
 f_1^\theta(p) &\triangleq \begin{bmatrix} 1 & \sqrt{3} \cos \theta \\ \sqrt{3} & -\cos \theta \end{bmatrix} p + \frac{1 + \cos \theta}{4} \begin{bmatrix} -\sqrt{3} \\ 1 \end{bmatrix}, \\
 f_2^\theta(p) &\triangleq \begin{bmatrix} -1 & -\sqrt{3} \cos \theta \\ \sqrt{3} & -\cos \theta \end{bmatrix} p + \frac{1 + \cos \theta}{4} \begin{bmatrix} \sqrt{3} \\ 1 \end{bmatrix}, \\
 f_3^\theta(p) &\triangleq \begin{bmatrix} -1 & \sqrt{3} \\ \sqrt{3} & 1 \end{bmatrix} p.
 \end{aligned}$$

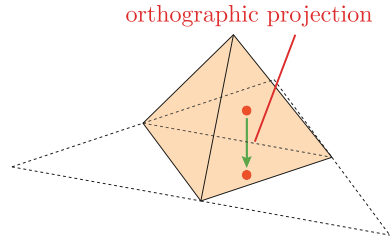
Since each subdomain \mathcal{D}_i^θ is defined as a closed set for all $i = 0, 1, 2, 3$, adjacent domains share the points on their boundaries. Note, however, that the map f^θ defined in Definition 7.2 has no ambiguity in that when $p \in (\mathcal{D}_i^\theta \cap \mathcal{D}_j^\theta)$ it follows that $f_i^\theta(p) = f_j^\theta(p)$ so that the point p on the intersection of the domains is mapped to the same point in \mathcal{D} .

Henceforth, for a subset $S \subset \mathcal{D}$, $f^\theta(S)$ denotes the set of points $f(p)$, $p \in \mathcal{D}$, which is also a subset of \mathcal{D} .

7.3 Tetrahedron Map

In this section, we consider the special case of the orthogonally projective triangle folding map. Specifically, consider the map f^θ for the case of $\theta = \cos^{-1} \frac{1}{3}$. This value is the critical value for the expression of the piecewise affine function and the folding in [2] of Fig. 7.3 is characterized by the tetrahedron as shown in Fig. 7.8. For this specialized map, we write f^Δ to denote $f^{\cos^{-1} \frac{1}{3}}$.

Fig. 7.8 Regular tetrahedron map (procedure [2] of Fig. 7.3). This is the special case of the orthogonal triangle folding map f^θ with $\theta = \cos^{-1} \frac{1}{3}$



Definition 7.3 (*Tetrahedron map*) For the point $p = [x, y]^T$ in the closed domain $\mathcal{D} \subset \mathbb{R}^2$, the tetrahedron map $f^\Delta : \mathcal{D} \rightarrow \mathcal{D}$ for the equilateral triangle is given by

$$f^\Delta(p) \triangleq f_i^\Delta(p), \quad p \in \mathcal{D}_i, \quad i = 2, 3, \tag{7.3}$$

where

$$\begin{aligned} f_2^\Delta(p) &\triangleq A_2^\Delta p + b_2^\Delta, \\ f_3^\Delta(p) &\triangleq A_3^\Delta p, \\ A_2^\Delta &\triangleq \begin{bmatrix} -1 & \frac{\sqrt{3}}{3} \\ \sqrt{3} & -\frac{1}{3} \end{bmatrix}, \quad b_2^\Delta \triangleq \frac{1}{3} \begin{bmatrix} \sqrt{3} \\ 1 \end{bmatrix}, \\ A_3^\Delta &\triangleq \begin{bmatrix} -1 & \sqrt{3} \\ \sqrt{3} & 1 \end{bmatrix}. \end{aligned}$$

7.3.1 Fixed Point and Periodic Point Analysis on the Boundary of \mathcal{D}

In this section, we restrict our attention on the boundary $\partial\mathcal{D}$ of the domain \mathcal{D} and provide analysis in regards to the fixed points and the periodic points. Specifically, note that the folding map f maps every point on $\partial\mathcal{D}$ onto $\partial\mathcal{D}$. In other words, the set $\partial\mathcal{D}$ is a positively invariant set with respect to f .

For the analysis presented in this section, we define the map $f_\partial^\Delta : \partial\mathcal{D} \rightarrow \partial\mathcal{D}$ as

$$f_\partial^\Delta(p) = f_i^\Delta(p), \quad p \in (\mathcal{D}_i \cap \partial\mathcal{D}), \quad i = 2, 3, \tag{7.4}$$

where $f_i^\Delta(\cdot), i = 2, 3$, are given by (7.4). Furthermore, for the statement of the following result, let the points A, B, C, D be placed on the boundary of \mathcal{D} as shown in Fig. 7.9.

Theorem 7.1 Consider the tetrahedron map f_∂^Δ given by (7.4). For $\partial\mathcal{D}$, let A, B, C, D denote the points shown in Fig. 7.9. Then the map $f_\partial^\Delta : \partial\mathcal{D} \rightarrow \partial\mathcal{D}$ satisfies the following properties:

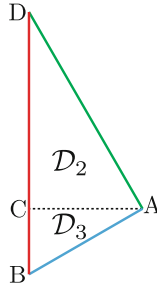


Fig. 7.9 Definition of the points A, B, C, D on the boundary of \mathcal{D}

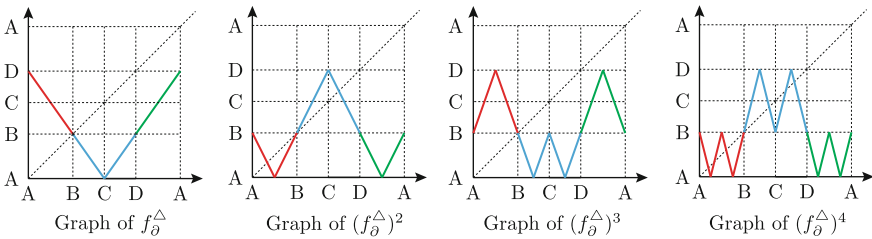


Fig. 7.10 The mapping relation of the points on the boundary of \mathcal{D} for the maps $f_{\theta}^{\Delta}, (f_{\theta}^{\Delta})^2, (f_{\theta}^{\Delta})^3,$ and $(f_{\theta}^{\Delta})^4$. The point B can be seen as a fixed point for the map $(f_{\theta}^{\Delta})^k, k \in \mathbb{N}$

1. For k even, the k -times composite map $(f_{\theta}^{\Delta})^k$ has $2^{k/2}$ fixed points on the edge A-B.
2. For k even, the k -times composite map $(f_{\theta}^{\Delta})^k$ has $2^{k/2}$ fixed points on the edge B-D.
3. For k even, the k -times composite map $(f_{\theta}^{\Delta})^k$ has $2^{k/2+1} - 1$ fixed points on $\partial\mathcal{D}$.
4. For k odd, the k -times composite map $(f_{\theta}^{\Delta})^k$ has a unique fixed point on $\partial\mathcal{D}$, which is the vertex B.

Proof The results can be shown from the relationship given in Fig. 7.10 where f_{θ} is surjective from $\partial\mathcal{D}$ to $\partial\mathcal{D}$. □

7.4 Extended Fixed Point and Periodic Point Analysis for Tetrahedron Map

7.4.1 Geometric Interpretation of the Triangle Folding Map

In this section, we provide characterization of the fixed and the periodic points of the tetrahedron map f^{Δ} over the domain \mathcal{D} and compute the Lyapunov exponent of the map. In the following, we give mathematical representation of the partitioned domains and characterize the relationship between the partitioned domains and the map f^{Δ} .

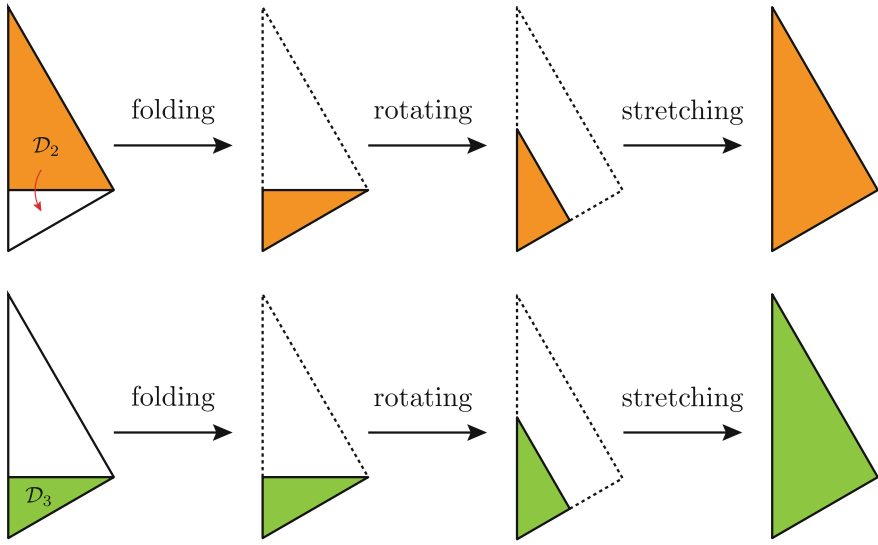


Fig. 7.11 Transition of \mathcal{D}_2 and \mathcal{D}_3 . For both of the domains, they are mapped to the domain \mathcal{D}

Definition 7.4 (Sequentially partitioned set by a sequence) For a given $k \in \mathbb{N}$, consider the collection of finite sequences \mathcal{S}_k given by

$$\mathcal{S}_k \triangleq \left\{ s = \{s_i\}_{i=0}^{k-1} : s_i \in \{2, 3\}, i = 0, 1, \dots, k-1 \right\}. \tag{7.5}$$

Then the subset \mathcal{D}_s , where $s = \{s_0, s_1, \dots, s_{k-1}\} \in \mathcal{S}_k$, is defined as

$$\mathcal{D}_s \triangleq \{p \in \mathcal{D}_{s_0} : f^\Delta(p) \in \mathcal{D}_{s_1}, (f^\Delta)^2(p) \in \mathcal{D}_{s_2}, \dots, (f^\Delta)^{k-1}(p) \in \mathcal{D}_{s_{k-1}}\}. \tag{7.6}$$

For simplicity of exposition, we write $\mathcal{D}_{ij\dots k}$ to denote $\mathcal{D}_{\{i,j,\dots,k\}}$.

Consider the partitioned domains for the map $(f^\Delta)^2$. Note that f^Δ maps \mathcal{D}_2 and \mathcal{D}_3 to \mathcal{D} (see Fig. 7.11).

In other words, by taking the inverse map in Fig. 7.11, we can characterize the partitioned domains for the map $(f^\Delta)^2$, which are shown in Fig. 7.12.

In a similar manner, it is possible to characterize the partitioned domains for the map $(f^\Delta)^k$ by applying the similar procedure [1] in Fig. 7.12 to the partitioned domains for the map $(f^\Delta)^{k-1}$. As an example, the partitioned domains for the map $(f^\Delta)^3$ is shown in Fig. 7.13.

In summary, the partitioned domains for $f^\Delta, (f^\Delta)^2, (f^\Delta)^3, (f^\Delta)^4$ are shown in Fig. 7.14.

Remark 7.1 According to this definition, the notation \mathcal{D}_i used in the previous sections stands for $\mathcal{D}_{\{i\}}$.

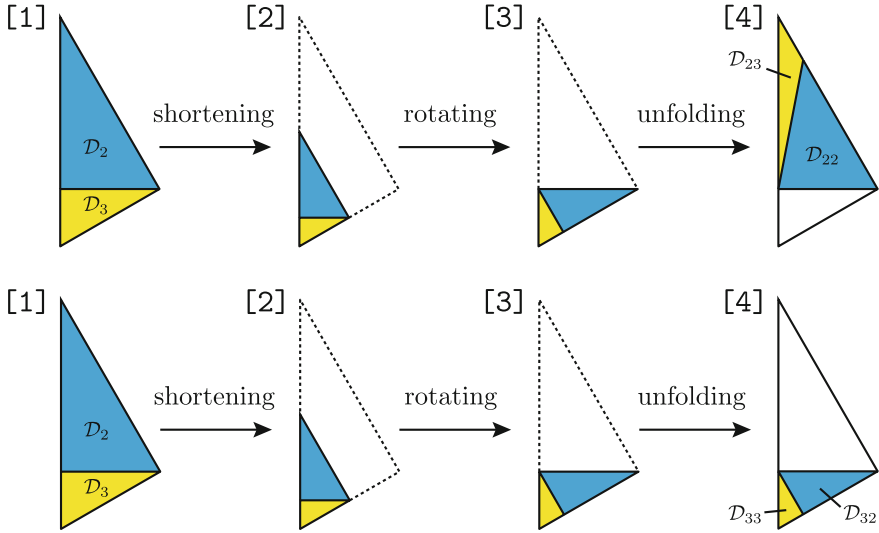


Fig. 7.12 Domain of $(f^\Delta)^2$, which are twice inverse maps of the domain \mathcal{D} . There are two cases to be mapped to the domain \mathcal{D}_2 (above) and \mathcal{D}_3 (below)

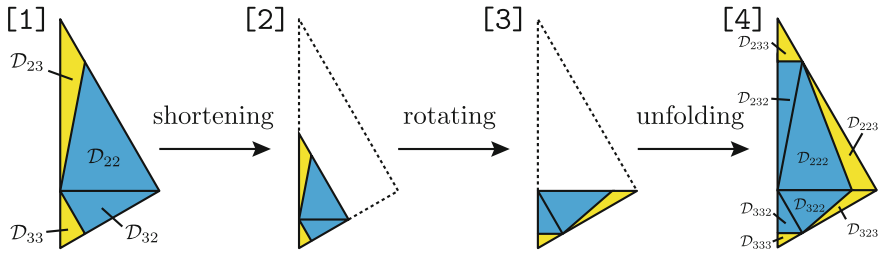


Fig. 7.13 Domain of $(f^\Delta)^3$. The domains $\mathcal{D}_{223}, \mathcal{D}_{233}, \mathcal{D}_{323}, \mathcal{D}_{333}$ in [4] are mapped to the domains \mathcal{D}_{23} and \mathcal{D}_{33} in [1] by f^Δ

Definition 7.5 Let $k, l \in \mathbb{Z}^+$ and let $u = \{u_0, u_1, \dots, u_{k-1}\} \in \mathcal{S}_k$ and $v = \{v_0, v_1, \dots, v_{l-1}\} \in \mathcal{S}_l$. Then the operation $\oplus : \mathcal{S}_k \times \mathcal{S}_l \rightarrow \mathcal{S}_{k+l}$ is defined as

$$u \oplus v \triangleq \{u_0, u_1, \dots, u_{k-1}, v_0, v_1, \dots, v_{l-1}\}. \tag{7.7}$$

Theorem 7.2 For any $s \in \mathcal{S}_k, k \in \mathbb{Z}^+$, it follows that

$$\Pi_2(\mathcal{D}_s) = \mathcal{D}_{s \oplus \{2\}}, \tag{7.8}$$

$$\Pi_3(\mathcal{D}_s) = \mathcal{D}_{s \oplus \{3\}}. \tag{7.9}$$

Next, we define a left shift operation for the sequence s .

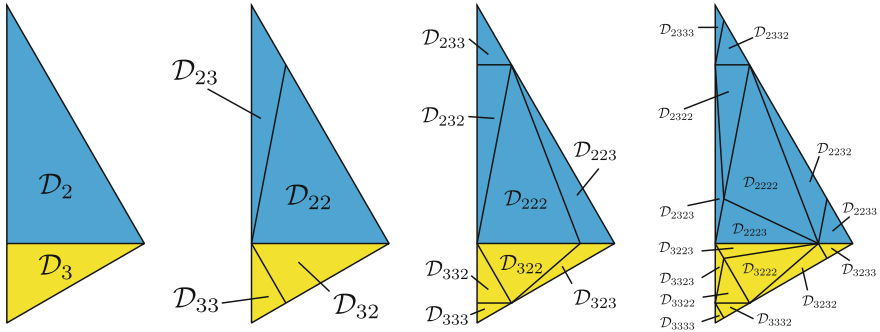


Fig. 7.14 Domains of $\mathcal{D}_{s_0, \dots, s_k}$ for $k = 1, 2, 3, 4$

Definition 7.6 (*Left shift operation of sequences*) For a given $k \in \mathbb{N}$ and the finite sequence $s = \{s_0, s_1, \dots, s_{k-1}\} \in \mathcal{S}$, let $i \in \mathbb{N}$ be $i < k$. The left shift operation for s is defined as the binary operation $\ll: \mathcal{S} \times \mathbb{N} \rightarrow \mathcal{S}$ given by

$$s \ll i \triangleq \{s_i, s_{i+1}, \dots, s_{k-1}\}. \tag{7.10}$$

This definition makes it possible to simply represent the tetrahedron map for the equilateral triangle.

Theorem 7.3 *For a given $k \in \mathbb{N}$ and the finite sequence $s = \{s_0, s_1, \dots, s_{k-1}\} \in \mathcal{S}$, let $i \in \mathbb{N}$ be $i < k$. Then it follows that*

1. $(f^\Delta)^i(D_s) = D_{s \ll i}$,
2. $(f^\Delta)^i(p) \in \mathcal{D}_{s \ll i}$, $p \in \mathcal{D}_s$.

Proof We show the case of $i = 1$ in (i) because the result of (i) can be shown by applying the case of $i = 1$ and the result of (ii) is immediate from (i).

Note from Definition 7.4 that

$$\begin{aligned} f(\mathcal{D}_s) &= f^\Delta \circ \Pi_{s_{n-1}} \circ \dots \circ \Pi_{s_1} \circ \Pi_{s_0}(\mathcal{D}) \\ &= f^\Delta \circ \Pi_{s_{n-1}} \circ \dots \circ \Pi_{s_1}(\mathcal{D}_{s_0}) \\ &= \Pi_{s_{n-1}} \circ \dots \circ \Pi_{s_1} \circ f^\Delta(\mathcal{D}_{s_0}). \end{aligned}$$

Note that $f^\Delta(\mathcal{D}_{s_0}) = \mathcal{D}$ for every $s_0 \in \{2, 3\}$. Hence, it follows that

$$f^\Delta(\mathcal{D}_s) = \Pi_{s_{n-1}} \circ \dots \circ \Pi_{s_1}(\mathcal{D}) = \mathcal{D}_{s \ll 1},$$

which completes the proof. □

The result (i) in Theorem 7.3 indicates the fact that applying the tetrahedron map f is equivalent to shifting left the subscript s of \mathcal{D}_s by 1, while (ii) suggests that the mapped point $(f^\Delta)^k(p)$ of $p \in \mathcal{D}$ by $(f^\Delta)^k$ may be estimated.

Theorem 7.4 (Grey code property) *Let $k \in \mathbb{Z}^+$. For the partitioned domains \mathcal{D}_s and $\mathcal{D}_{s'}$ for the map $(f^\Delta)^k$ with $s' = \{s'_0, s'_1, \dots, s'_{k-1}\} \in \mathcal{S}_k$, there exists $0 \leq \alpha \leq k-1$ such that*

$$s_\alpha \neq s'_\alpha, \quad (7.11)$$

$$s_i = s'_i, \quad i \neq \alpha, \quad 0 \leq i \leq k-1. \quad (7.12)$$

Proof The result is proven by invoking induction. \square

7.4.2 Periodic Points of the Tetrahedron Map

The main result of this section is shown in Theorems 7.5 and 7.6 below. Before stating the result, we need to provide several preliminary lemmas.

Lemma 7.1 *Let g^Δ denote $(f^\Delta)^k$. Then, for any $s \in \mathcal{S}_k$, $k \in \mathbb{Z}^+$, the map $g_{\text{dom}(\mathcal{D}_s)}^\Delta$ is bijective.*

Lemma 7.2 *Let $l \in \mathbb{Z}$ and $k \in \mathbb{Z}^+$ be such that k is even and $0 \leq l \leq k$, and let $s = \{s_0, s_1, \dots, s_{k-1}\} \in \mathcal{S}_k$. Then it follows that*

$$A_{s_{k-1}}^\Delta A_{s_{k-2}}^\Delta \dots A_{s_0}^\Delta = 2^k \begin{bmatrix} 1 & 0 \\ 0 & (-1/3)^l \end{bmatrix}. \quad (7.13)$$

Theorem 7.5 *The k -times tetrahedron map $(f^\Delta)^k : \mathcal{D} \rightarrow \mathcal{D}$ has a unique fixed point on \mathcal{D}_s , $s \in \mathcal{S}_k$, $k \in \mathbb{Z}^+$.*

Proof The fixed point of the map $(f^\Delta)^k$ on \mathcal{D}_s can be obtained by solving the equation $g^\Delta = (f^\Delta)^k(p) = p$ or, equivalently,

$$A_{s_{k-1}}^\Delta A_{s_{k-2}}^\Delta \dots A_{s_0}^\Delta p + C = p. \quad (7.14)$$

Now, since

$$\det \left(A_{s_{k-1}}^\Delta A_{s_{k-2}}^\Delta \dots A_{s_0}^\Delta - I \right) \neq 0, \quad (7.15)$$

it follows that (7.14) has a unique solution p . \square

Lemma 7.3 *Let p be the fixed point for $(f^\Delta)^k$. Then there do not exist two distinct sequences α and β of length k such that $p \in \mathcal{D}_\alpha$ and $p \in \mathcal{D}_\beta$.*

Theorem 7.6 *The map $(f^\Delta)^k$ possesses 2^k fixed points on \mathcal{D} .*

Proof It follows from Theorem 7.5 and Lemma 7.3 that $(f^\Delta)^k$ possesses a fixed point on the boundary or the interior of \mathcal{D}_s . Note that these fixed points are not shared by 2 different domains. Hence, the number of fixed points is equal to the number of the partitioned domains. \square

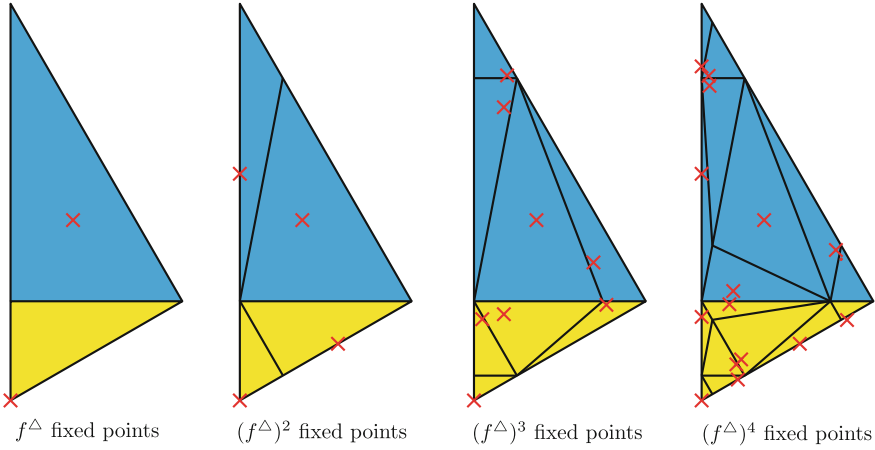


Fig. 7.15 Domain separation and fixed points of f^Δ , $(f^\Delta)^2$, $(f^\Delta)^3$, $(f^\Delta)^4$. There are 2 fixed points for the map f^Δ (left). Similarly, the fixed points for the map $(f^\Delta)^2$ are shown in the middle left figure but the ones in the left figure are also included in the figure. The same comment applies to the figures for $(f^\Delta)^3$ and $(f^\Delta)^4$

7.4.3 Chaos by the Tetrahedron Map

In this section, we show that the tetrahedron map exhibits chaotic behavior.

Theorem 7.7 *The tetrahedron map $f^\Delta : \mathcal{D} \rightarrow \mathcal{D}$ is topologically transitive on \mathcal{D} and possesses dense periodic points on \mathcal{D} .*

Hence, the tetrahedron map f^Δ exhibits chaotic behavior on \mathcal{D} .

Figure 7.15 shows the partitioned domains and the corresponding fixed points for f^Δ , $(f^\Delta)^2$, $(f^\Delta)^3$, $(f^\Delta)^4$.

Theorem 7.8 *Let $k \in \mathbb{Z}^+$ and let $i \leq k$ be an integer. Furthermore, define the circular function $\text{Circ}_i^k : \mathcal{S}^k \rightarrow \mathcal{S}^k$ given by*

$$\text{Circ}_i^k(s) \triangleq \{s_i, s_{i+1}, \dots, s_{k-1}, s_0, s_1, \dots, s_{i-1}\}. \tag{7.16}$$

Then there exists $s \in \mathcal{S}_k$ such that

$$\begin{aligned} f^\Delta(x_s) &= x_{\text{Circ}_1^k(s)}, \\ f^\Delta(x_{\text{Circ}_1^k(s)}) &= x_{\text{Circ}_2^k(s)}, \\ &\vdots \\ f^\Delta(x_{\text{Circ}_{k-1}^k(s)}) &= x_{\text{Circ}_k^k(s)} = x_s, \end{aligned}$$

where x_s denotes a fixed point for the map $(f^\Delta)^k$.

Proof It suffices to show $f^\Delta(x_s) = x_{\text{Circ}_1^k(s)}$. For any $s = \{s_0, s_1, \dots, s_{k-1}\} \in \mathcal{S}_k$, it follows that

$$f_{s_{k-1}}^\Delta \circ f_{s_{k-2}}^\Delta \circ \dots \circ f_{s_0}^\Delta(x_s) = x_s,$$

and hence

$$f_{s_0}^\Delta \circ f_{s_{k-1}}^\Delta \circ f_{s_{k-2}}^\Delta \circ \dots \circ f_{s_0}^\Delta(x_s) = f_{s_0}^\Delta(x_s).$$

On the other hand, it follows that for $x_{\text{Circ}_1^k(s)}$,

$$f_{s_0}^\Delta \circ f_{s_{k-1}}^\Delta \circ f_{s_{k-2}}^\Delta \circ \dots \circ f_{s_1}^\Delta(x_{\text{Circ}_1^k(s)}) = x_{\text{Circ}_1^k(s)}.$$

By comparing the above two equations, we obtain

$$f_{s_0}^\Delta(x_s) = x_{\text{Circ}_1^k(s)},$$

and hence $f^\Delta(x_s) = x_{\text{Circ}_1^k(s)}$. □

Corollary 7.1 *The number T_k of periodic orbits with the fundamental period k is given by $T_1 = 2$ and*

$$T_k = \frac{1}{k} \left(2^k - \sum_{i \in \mathcal{M}_k} iT_i \right). \tag{7.17}$$

Figure 7.16 shows the periodic orbits of period 1, 2, 3, and 4.

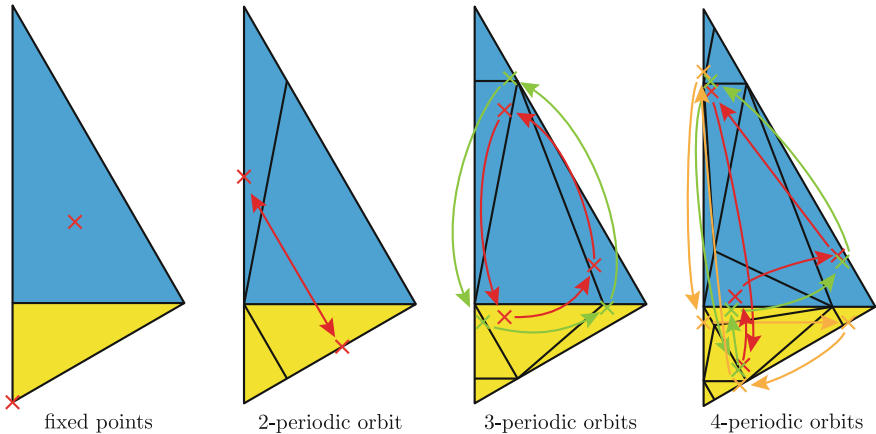


Fig. 7.16 Domain separation and true periodic orbits of $f^\Delta, (f^\Delta)^2, (f^\Delta)^3, (f^\Delta)^4$. There are 2, 1, 2, 3 periodic orbits for the periods 1, 2, 3, and 4, respectively

7.5 Conclusion

In this article, we proposed a simple folding map associated with the equilateral triangle and provided intensive analysis for the case where the folding leads to form the tetrahedron. Specifically, we showed that each partitioned domain possesses a unique fixed point for the map $(f^\Delta)^k$ and the labels of the domains satisfy the grey code property. Furthermore, we showed that when θ is less than the value of $\cos^{-1} \frac{1}{3}$, the f^Δ exhibits chaotic behavior in the sense of Devaney. Future works include investigating the connections and the differences between the folding map and the well-known horseshoe map, which also has the notion of ‘folding’ in its operation.

References

1. Amaral, G.F.V., Letellier, C., Aguirre, L.A.: Piecewise affine models of chaotic attractors: the Rossler and Lorenz systems. *Interdisc. J. Nonlinear Sci., Chaos* **16** (2006)
2. Chen, G., Yu, X.: *Chaos Control: Theory and Applications*. Springer, Berlin (2003)
3. Devaney, R.: *An Introduction to Chaotic Dynamical Systems*. Addison-Wesley Studies in Nonlinearity. Westview Press, Reading (2003)
4. Guckenheimer, J., Holmes, P.: Nonlinear oscillations dynamical systems, and bifurcations of vector fields. *J. Appl. Mech.* **51** (1984)
5. Guckenheimer, J., Holmes, P.: *Nonlinear Oscillations, Dynamical Systems, and Bifurcations of Vector Fields*. Springer, New York (1983)
6. Ishikawa, T., Hayakawa, T.: Chaotic behavior of the folding map on the equilateral triangle. In: *Proc. Sympos. Nonlin. Contr. Syst.*, 767–772 (2013)
7. May, R.M.: Simple mathematical models with very complicated dynamics. *Nature* **261**(5560), 459–467 (1976)
8. Melnikov, V.K.: On the stability of the center for time periodic perturbations. *Trans. Moscow Math.* **12**, 1–57 (1963)
9. Mielke, A., Holmes, P., O’Reilly, O.: Cascades of homoclinic orbits to, and chaos near, a hamiltonian saddle-center. *J. Dyn. Diff. Eqn.* **4**(1), 95–126 (1992)
10. Nishimura, J., Hayakawa, T.: Chaotic dynamics of orthogonally projective triangle folding map. In: *Proc. IEEE Conf. Dec. Contr.*, 813–815 (2014)
11. Robinson, C.: *Dynamical Systems: Stability, Symbolic Dynamics, and Chaos*. CRC Press, Boca Raton (1998)
12. Smale, S.: *Diffeomorphisms With Many Periodic Points*. Department of Mathematics, Columbia University, New York (1963)
13. Smale, S.: *The Mathematics of Time: Essays on Dynamical Systems, Economic Processes and Related Topics*. Springer, New York (1980)